

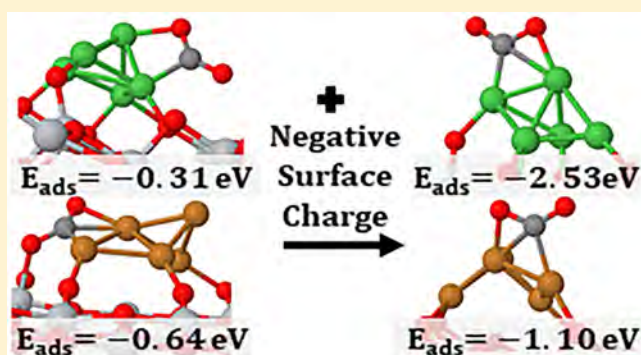
CO₂ Activation on TiO₂-Supported Cu₅ and Ni₅ Nanoclusters: Effect of Plasma-Induced Surface Charging

A. Jafarzadeh,*¹ K. M. Bal,¹ A. Bogaerts,¹ and E. C. Neyts¹

Research group PLASMANT, Department of Chemistry, University of Antwerp, Universiteitsplein 1, Wilrijk, 2610 Antwerp, Belgium

Supporting Information

ABSTRACT: Surface charging is an often overlooked factor in many plasma–surface interactions and in particular in plasma catalysis. In this study, we investigate the effect of excess electrons induced by a plasma on the adsorption properties of CO₂ on titania-supported Cu₅ and Ni₅ clusters using spin-polarized and dispersion-corrected density functional theory calculations. The effect of excess electrons on the adsorption of Ni and Cu pentamers as well as on CO₂ adsorption on a pristine anatase TiO₂(101) slab is studied. Our results indicate that adding plasma-induced excess electrons to the system leads to further stabilization of the bent CO₂ structure. Also, dissociation of CO₂ on charged clusters is energetically more favorable than on neutral clusters. We hypothesize that surface charge is a plausible cause for the synergistic effects sometimes observed in plasma catalysis.



INTRODUCTION

Plasma catalysis^{1,2} holds promise for many environmental^{3–8} and industrial^{9,10} applications. Combining a plasma with a catalyst induces a complex reciprocal interaction, which in some cases leads to synergistic effects that improve the efficiency of the catalytic reactions. However, the underlying reasons for the synergy in plasma catalysis remain unknown. Reaction promotion in the catalytic removal of NO_x,¹¹ higher CO₂ conversion,¹² decrease in the energy barrier for dry reforming of methane,¹³ and increased treatment efficiency on *Escherichia coli* cells in aqueous media¹⁴ have been reported as a result of synergistic effects in plasma catalysis.

Plasma is an ionized gas that consists of different interacting species such as electrons, ions, neutral atoms, and vibrationally and electronically excited species. The presence of these species makes the plasma a highly reactive but nonselective environment that is very suitable for combining with a catalyst.² In particular, the plasma leads to a modification of the gas phase (and hence the reactants), while still allowing for a (relatively) low temperature. The contribution of all of the specific plasma factors strongly depends on the type of plasma and the working conditions and has been studied extensively. The mechanisms of plasma-induced changes in the structural and electronic properties of the catalyst remain largely unresolved. To unravel (some of) the mechanisms underlying plasma–catalyst interactions, we need to narrow down the complexity of the system by focusing on a specific factor and its effect on the whole plasma–catalytic process. Comple-

mentary to experiments, computer simulations are ideally suited for this.

A catalyst surface becomes inevitably charged upon interaction with a plasma. The accumulated surface charge can alter the electronic and geometric structures of the catalyst, consequently leading to a change in the kinetics of the whole catalytic reaction. Even changes in the activity of the different geometric structures of a catalyst are generally ascribed to differences in their electronic structures.¹⁵ Hence, by considering the electronic properties of the catalyst during its interaction with a plasma, one can gain information about the effect of plasma-induced surface charging on catalytic reactions.

The effect of surface charging, for instance due to a plasma, is important in heterogeneous catalysis and in particular when transition metal clusters are deposited on oxide surfaces. Excess electrons accumulated on the oxide surface can alter the electronic structure and adsorption properties of the supported transition metal nanoparticles. Although there have been experimental^{16,17} and theoretical^{18,19} investigations on the effect of plasmas in heterogeneous catalysis, and studies have been carried out on the deposition of metal clusters on oxide surfaces without a plasma,^{20–22} the effect of plasma-induced excess electrons on the deposition of metal clusters and their catalytic properties has been scarcely investigated. Both nickel

Received: December 7, 2018

Revised: February 14, 2019

Published: February 21, 2019

and copper are widely used in heterogeneous catalysis, for instance, for CO₂ conversion^{18,23,24} for forming value-added products like methanol. We here choose to study Ni and Cu pentamers. First, these clusters can be synthesized and are actually used in the catalysis community. Further, because of their small size, they require less material, making them cheaper (per unit surface area) and possibly more environmentally friendly. Finally, considering the limited number of possible isomers, their fluxionality (in gas phase) is much lesser than that of larger clusters, which makes them computationally tractable.

In this study, we report the role of excess electrons in (1) the adsorption of Ni₅ and Cu₅ clusters on an anatase TiO₂(101) slab as test systems, (2) the adsorption of an adsorbate molecule (CO₂) on the stoichiometric surface of anatase TiO₂(101), (3) the adsorption of a CO₂ molecule on TiO₂-supported Ni₅ and Cu₅ clusters, and (4) the dissociation of the CO₂ molecule.

As a reducible oxide, TiO₂ is an interesting candidate to investigate the effects of surface charging. Among the various polymorphs of titania, anatase has been widely used in modeling catalytic reactions.^{20–22,25,26} The (101) plane of anatase (a-TiO₂) has been chosen for the adsorption of the metal clusters because of its high thermodynamic stability.²¹

■ COMPUTATIONAL DETAILS

All calculations have been carried out based on the spin-polarized density functional theory (DFT) by using the Quickstep²⁷ module of the CP2K²⁸ package. This module mainly employs localized Gaussian orbitals and auxiliary plane waves as a dual basis for expanding the Kohn–Sham orbitals. Double- ζ valence plus polarization basis sets, which are optimized from molecular interactions (MOLOPT),^{29,29} combined with a plane wave basis set with 800 Ry cutoff have been used for the calculations. Goedecker–Teter–Hutter pseudopotentials^{30,31} are used for describing the inner shell electrons; for C, O, Cu, Ti, and Ni atoms, 4, 6, 11, 12, and 18 valence electrons are explicitly considered, respectively. The general gradient approximation Perdew–Burke–Ernzerhof³² functional is applied for treating electron exchange and correlation effects. Dispersion interactions are included through Grimme’s D3 approximation along with Becke–Jonsson damping.^{33,34} The Broyden–Fletcher–Goldfarb–Shanno scheme is used for geometry optimization where a maximum force of 0.02 eV/Å has been set for the relaxation of atoms. The k -point sampling is limited to the Γ -point only, and the Hirshfeld-I scheme³⁵ is used for charge analysis of interactions between the adsorbates and the slab surface.

Lattice parameters of bulk anatase TiO₂ ($a = b = 3.7845$ Å and $c = 9.5143$ Å)³⁶ were used for creating the surface slabs. A slab of anatase (101) with dimensions of $10.239 \times 11.3535 \times 30.00$ Å³ (1×3 supercell) consisting of six (O–Ti–O) trilayers and containing 108 atoms (Figure 1) was used for the calculations. To mimic the bulk-like structure, we fixed the bottom layers of the support in a first set of calculations. This, however, also leads to interference in the excess electrons’ localization pattern. Thus, we also examined a fully relaxed structure, with no atoms frozen. The results with the fixed layers are mainly provided in the Supporting Information (SI); we here mainly focus on the results achieved without applying any constraint on the relaxation of the atoms. Calculations for the metal clusters and the CO₂ molecule in gas phase have been carried out in a box of $15 \times 15 \times 15$ Å³ dimensions.

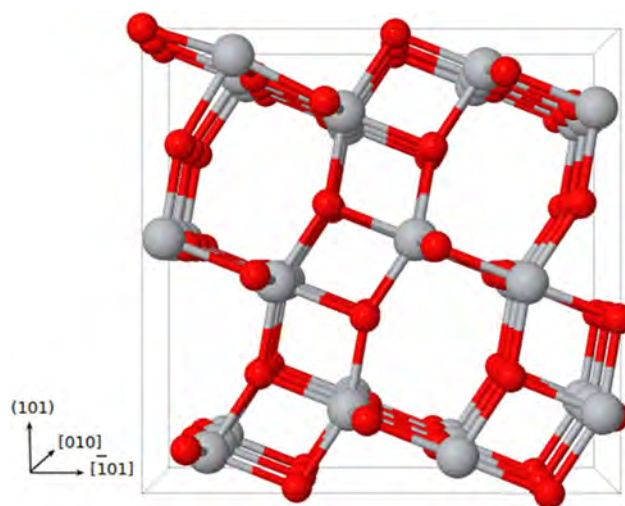


Figure 1. (1×3) Supercell of anatase TiO₂(101).

For the treatment of charged configurations, we applied our recently proposed method³⁷ suitable for modeling plasma–surface interactions. In this approach, we use a positive countercharge located far from the surface (in the z -direction) without assigning a local basis set to it. Thus, the electron density is not allowed to be distributed around the ion, but rather it will be localized on the surface. This is an ideal approach for modeling the effect of plasma-induced excess electrons on the surface of a catalyst, because it explicitly incorporates both the negative charging from excess electrons as well as polarization effects and electric fields arising from positively charged ions in the plasma sheath region in the gas phase.

Electrostatic interactions were described with the Martyna–Tuckerman (MT) Poisson solver,³⁸ which requires the z -component of the cell size to be very large (100 Å) for charged configurations. The MT solver allows one to impose full periodicity along the surface slab (in the xy plane), mimicking a semi-infinite catalyst surface, while simultaneously removing periodicity along the z direction. As such, unphysical interactions of the slab with itself are avoided, which would otherwise result in significant computational artifacts when dealing with charged surfaces.³⁹

We employed DFT + U ^{40,41} calculations for cross-checking the results, while accounting for the strong onsite Coulomb interactions. By using this approach, the self-interaction effect for Ti d-orbitals will be corrected by Hubbard’s U parameter. This parameter is set to 5 eV for Ti atoms. Considering the small number of atoms in clusters studied in this work, and negligible impact of their self-interaction on the results, no Hubbard parameter is applied to the d-orbitals of Ni and Cu atoms. Considering that DFT + U provides a better picture for electron localization on support cations, we referred to the projected density of states (PDOS) and spin density diagrams obtained by the DFT + U calculations.

We investigated the effect of charge in two ways: First, reoptimization of the neutral structure after adding an excess electron to the system, and second, optimization of the initially negatively charged configuration. After finding the most stable mode for both neutral and charged configurations, we made a comparison between the corresponding adsorption energies and other properties for the neutral and negatively charged structures.

Adsorption energies of clusters on anatase are calculated based on eq 1, where E_{cluster} is the total energy of the Ni₅/Cu₅ clusters, $E_{\text{slab+cluster}}$ is the total energy of the complex (consisting of cluster and surface), and E_{slab} is the total energy of the bare slab

$$E_{\text{adsorption}} = E_{\text{slab+cluster}} - E_{\text{cluster}} - E_{\text{slab}} \quad (1)$$

Similarly, the adsorption energy of CO₂ on the supported cluster is calculated as follows

$$E_{\text{adsorption}} = E_{\text{complex+molecule}} - E_{\text{complex}} - E_{\text{molecule}} \quad (2)$$

Thermal and zero-point energy calculations are not considered.

RESULTS AND DISCUSSION

Adsorption of Ni₅ and Cu₅ Clusters on the Anatase (101) Surface. To investigate the adsorption of Cu₅ and Ni₅ on the TiO₂ surface, we first optimized their structures in the gas phase, as described in the SI. Then, the clusters were deposited on the neutral anatase (101) surface and their adsorption energies were calculated. Subsequently, one electron was added to this configuration, and the system was reoptimized. This allowed us to compare the adsorption properties of each metal cluster in the neutral and charged systems. Similar to the gas phase calculations, we explored five initial structures with different orientations of the cluster adsorbing on the surface. Then we examined the most stable orientation in five different adsorption sites. The most stable configurations found for the adsorption of Ni₅ and Cu₅ clusters are shown in Figure 2, whereas the unstable adsorption modes are provided in the SI. We acknowledge that this procedure does not guarantee finding the global minimum.

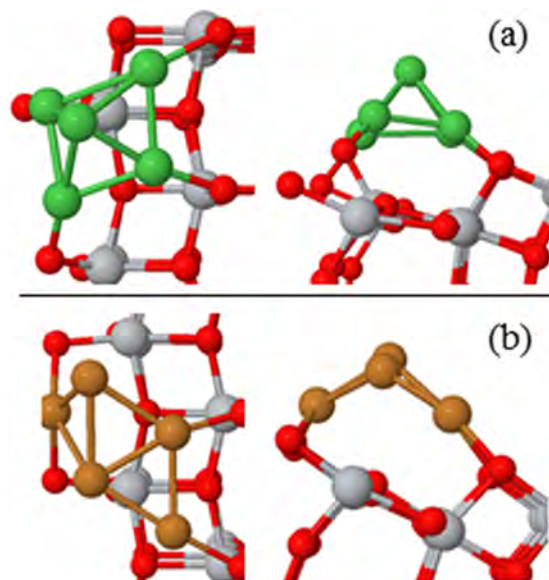


Figure 2. Top and side views of the most stable configurations of (a) Ni₅ and (b) Cu₅ clusters on the anatase TiO₂(101) slab.

Upon adsorption, hardly any change in the shape of the Ni₅ cluster is seen. Adsorption of the Ni₅ cluster on the anatase surface changes the electronic structure of the support such that the Ni d-orbitals fill the band gap of the TiO₂ semiconductor (see the SI) in agreement with the literature.^{42,43} Population analysis based on the Hirshfeld scheme shows that during the adsorption of Ni₅, there is a

charge transfer from the support to the cluster. For the gas phase Ni₅ cluster, the total spin moment ($n_{\alpha} - n_{\beta}$) is $2 \mu_{\text{B}}$ (triplet state), which changes to $3.1 \mu_{\text{B}}$ upon adsorption. Also, the accumulated net charge of $-0.893 |e|$ on the Ni₅ cluster shows that there is a significant charge transfer between the cluster and the surface, which leads to a high adsorption energy of -5.72 eV. This electron transfer from the support to the cluster leaves the support with one unpaired electron as can be seen from the spin density isosurfaces (Figure 3a).

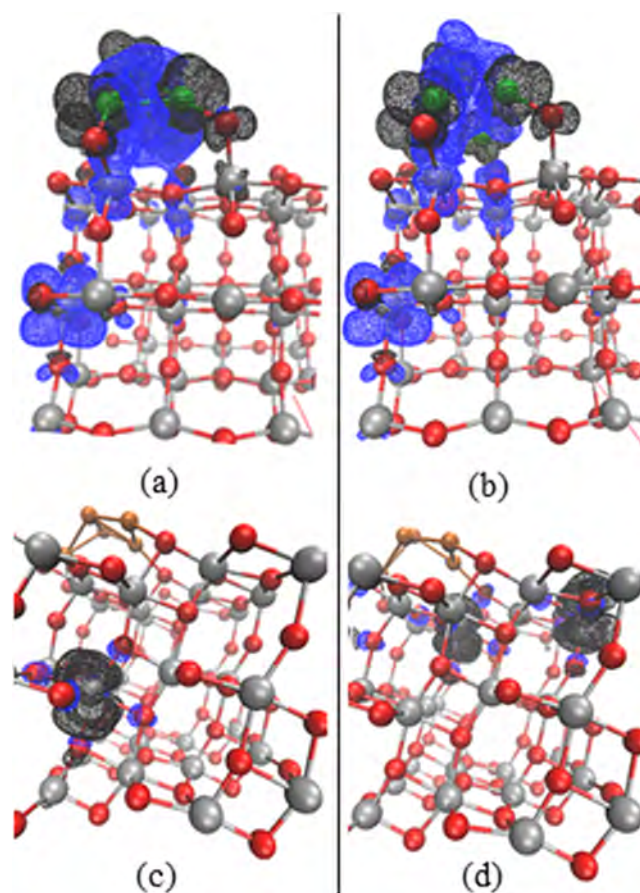


Figure 3. Spin density isosurfaces for (a) neutral Ni₅/TiO₂, (b) charged Ni₅/TiO₂, (c) neutral Cu₅/TiO₂, and (d) charged Cu₅/TiO₂ structures. The black and blue lobes correspond to spin up and spin down, respectively. Isovalues are set to ± 0.001 e/Å³.

Upon adsorption, the Cu₅ cluster changes its original planar configuration to a more three-dimensional structure, facilitating strong interaction between the cluster and the oxide surface with an adsorption energy of -4.29 eV. In comparison with Ni₅, the d-orbitals of the Cu₅ cluster partially lie in the TiO₂ band gap with a tendency to be located near the valence band (see the SI). The charge transfer direction between the support and the cluster is different for Ni₅ and Cu₅. The Cu₅ has a total spin moment of $2 \mu_{\text{B}}$ (doublet state) in the gas phase, which changes to 0 after its adsorption on the support surface. During the adsorption, one unpaired electron in the Cu₅ cluster is transferred to the support. From Figure 3c, we can see that the transferred electron localizes on the subsurface Ti atom of the support.

After adding an excess electron to the relaxed neutral structures and reoptimizing, no change in the adsorption mode is seen. Changes in adsorption energies as described below can

therefore (mostly) be attributed to the effect of the negative charge (Figure 4). Adding a single excess electron to the

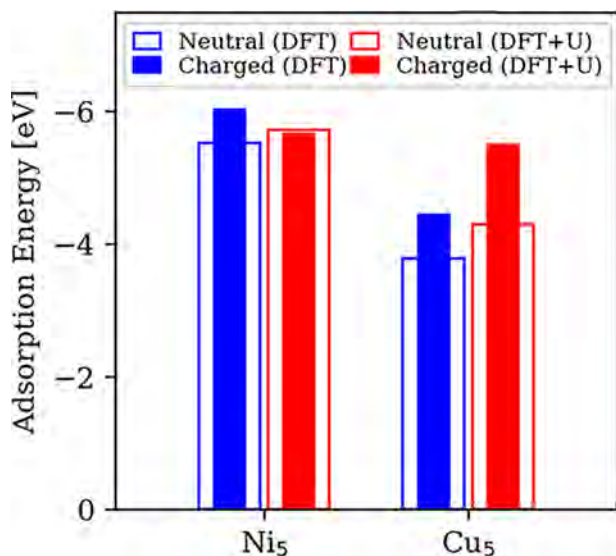


Figure 4. Adsorption energies of Ni₅ and Cu₅ clusters on anatase TiO₂(101).

surface model leads to an electron density of $8.6 \times 10^{17} \text{ m}^{-2}$ or a surface charge density of -0.137 C/m^2 , which is in the same order of experimental estimates of plasma-deposited charge densities on dielectrics⁴⁴ and 4 times higher than that reported in recent particle-in-cell/Monte Carlo collision PIC/MCC simulations for plasma in contact with dielectric surfaces or catalyst pores.⁴⁵

From the spin density analysis (Figure 3b), we can see that for the charged Ni₅ structure, the added electron is mostly localized on the Ni cluster, changing its net charge to $-1.643 |e|$ and also the total net spin moment to $2.2 \mu_B$. This gives rise to a change in the adsorption energy of the cluster by $+0.06 \text{ eV}$, amounting to an adsorption energy of -5.66 eV . However, in Figure 4, the DFT result without *U* correction shows that upon charging, the adsorption energy decreases by -0.51 eV , which is mostly because of the failure in localization of the excess electron.

In contrast, upon negatively charging the surface, no spin polarization on the Cu₅ is seen, which means that the added electron is not localized on the cluster (i.e., the net spin moment of the cluster remains 0). Instead, as can be seen from Figure 3d, the presence of excess electrons leads to a change in the localization of the previously transferred electron. Eventually, two electrons are localized on the surface of the support, which decreases the adsorption energy by 1.20 eV for the Cu₅ cluster, amounting to an adsorption energy of -5.49 eV . A detailed summary of the changes in the net spin moment and partial charges of the atoms for both neutral and charged structures is provided in the SI.

These results highlight the different effects of excess charge on the adsorption properties of Cu and Ni pentamers. Methodologically, these results also show that depending on the localization procedure of the excess electron, its effect on the stabilization of the adsorbed metal clusters can be different. Furthermore, it is seen that for fully relaxed systems, when using DFT calculations without considering onsite Coulomb

interactions, it is difficult to describe the effect of excess electrons on the stability of the metal clusters.

CO₂ Adsorption on Anatase TiO₂(101). CO₂ adsorption on neutral anatase was previously studied by DFT.^{43,44,46} In this study, our aim is to investigate the effect of plasma-induced excess electrons on the adsorption of CO₂ on both the bare surface and on titania-supported Ni₅ and Cu₅ clusters. We will focus on the two most stable configurations for the adsorption of CO₂ on the anatase (101) surface, as shown in Figure 5.

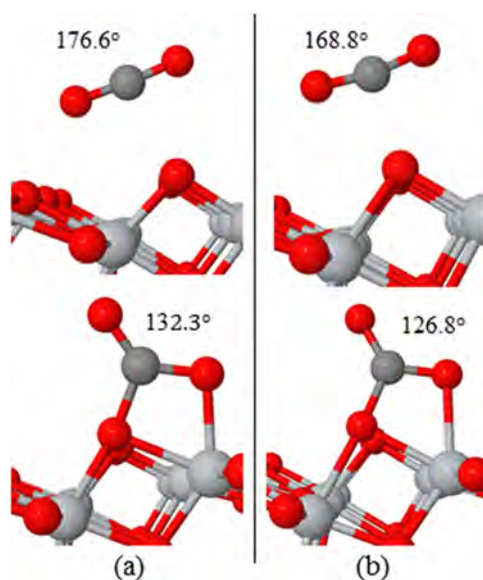


Figure 5. Most stable configurations for the linear and bent CO₂ structures adsorbing on the TiO₂(101) surface: (a) neutral and (b) charged configurations.

We first kept the three layers of the TiO₂ slab frozen in their bulk structure to allow for a direct comparison between the results for neutral structures and the literature. For the linear configuration, CO₂ was found to adsorb on the neutral surface with adsorption energies of -0.44 and -0.51 eV using DFT and DFT + *U*, respectively. The bent structure shows an adsorption energy of -0.03 eV using DFT, whereas DFT + *U* yields an adsorption energy of -0.18 eV . It can be seen that the results obtained using DFT + *U* are in agreement with the values of -0.48 eV for linear and -0.16 eV for carbonate-like structures, as reported by Sorescu et al.⁴⁴ Iyemperumal et al.⁴³ reported values of -0.40 and -0.09 eV for the most stable linear and bent structures, respectively. Results for both neutral and charged structures of CO₂ adsorption on bare TiO₂ (with fixed bottom layers) are shown in Figure 6a.

By removing the constraint on the bottom layers of the slab, the electron distribution is unbiased, which permits a reliable comparison between the neutral and charged structures. The results for fully relaxed systems are provided in Figure 6b. As we can see from this figure, the trends are maintained, although there are quantitative differences in the adsorption energies achieved for the system with fixed layers.

By adding charge to the system, both adsorption modes essentially maintain their structure. In the linear adsorption mode, the effect of excess charge on the adsorption energy is less pronounced. In this case, there is no mixing between the states of the molecule and the surface, such that the (small) increase in the adsorption energy of the linear CO₂ can be

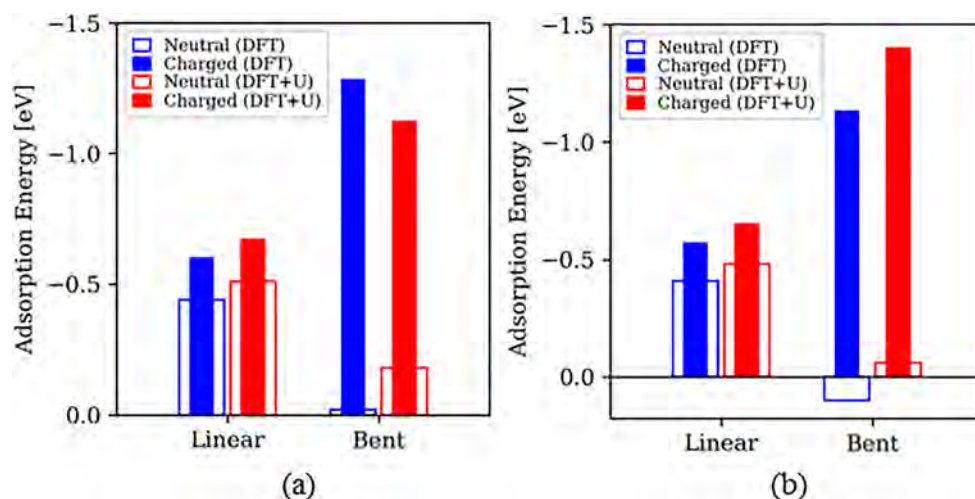


Figure 6. CO₂ adsorption energy for both linear and bent structures on neutral and charged configurations of anatase (101): (a) structures with three bottom layers kept frozen and (b) fully relaxed structures.

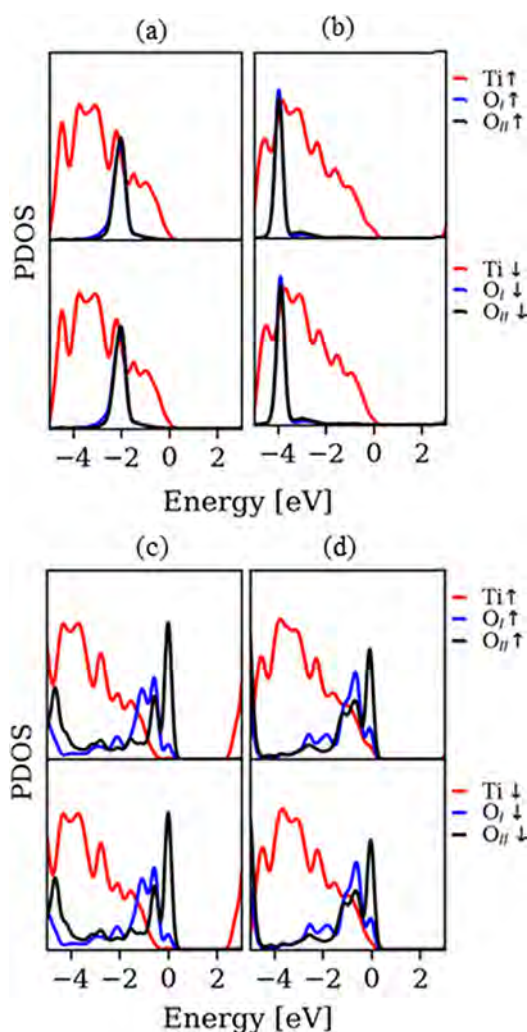


Figure 7. Projected density of states for the adsorption of a CO₂ molecule on TiO₂: (a) linear–neutral, (b) linear–charged, (c) bent–neutral, and (d) bent–charged structures. O_I and O_{II} are oxygen atoms of the CO₂ molecule. Up/down spin states are shown with up/down arrows.

Table 1. Bond Lengths and Adsorption Energies of CO₂ with Both Linear and Bent Structures in Neutral and Charged Configurations

method	structure	$r(\text{C}-\text{O})$	α (OCO)	E_{ads} (eV)
DFT	gas phase	1.17, 1.17	180	
	bent (neutral)	1.20, 1.32	131.6	0.10
	bent (charged)	1.23, 1.32	126.4	−1.13
	linear (neutral)	1.17, 1.18	177.2	−0.41
	linear (charged)	1.18, 1.18	169.9	−0.57
DFT + U	bent (neutral)	1.20, 1.32	132.3	−0.06
	bent (charged)	1.23, 1.32	126.8	−1.40
	linear (neutral)	1.17, 1.18	176.6	−0.48
	linear (charged)	1.18, 1.18	168.8	−0.65

attributed to polarization effects. In this case, electrostatic Coulomb forces between the positive C atom and the negatively charged surface will lead to an improvement in the adsorption energy. The PDOS of the linear adsorption mode for both neutral and charged structures (Figure 7a,b) reveals that upon charging, the states of both oxygen atoms of the CO₂ molecule are shifted toward lower energies and this leads to a small improvement in the stabilization of the molecule.

For the bent structure, there is a substantial increase in the adsorption energy upon charging, to −1.13 and −1.40 eV in DFT and DFT + U, respectively, which is also reflected in the partial charges of CO₂ in the neutral and charged configurations: the partial charges on oxygen atoms of the CO₂ molecule change from −0.862 |e| and −0.624 |e| (neutral system) to −1.028 |e| and −0.728 |e| (charged system), respectively. Considering that the surface Ti atom bonded to the oxygen atom of the CO₂ molecule has preserved its net charge from the neutral configuration, we can see that the increase in adsorption energy is mainly due to the change in the partial charge of the molecule. This is consistent with the PDOS diagrams (Figure 7d) of the charged configuration, showing a shift in the DOS of the oxygen atoms of CO₂ toward the valence band, facilitating the pronounced mixing with orbitals of the surface Ti atoms, in comparison with the neutral case.

Table 1 shows the effect of charge on the adsorption energy of the two most stable modes of CO₂ on titania achieved by

DFT and DFT + *U*. The same trend is clear from the results shown in Figure 6.

Transformation of the linear to the bent structure thus seems essential for CO₂ activation. It is clear from the results that adding a plasma-deposited excess electron to the system changes the most stable structure of the CO₂ adsorbed on titania surface from a linear to a bent configuration, which makes the activation of the CO₂ molecule thermodynamically more favorable. Correspondingly, we also analyzed changes in the C–O bond length and in the O–C–O bond angle as a result of negatively charging the surface. In Table 1, we summarize the results for the effect of charge on bond lengths and angles. It can be seen that the presence of excess charge has an impact on bending the CO₂ molecule, whereas the effect on the C–O bond elongation is limited.

CO₂ Adsorption on Supported Clusters. For the adsorption of CO₂ on titania-supported clusters, various initial modes were examined. In this case, we optimized each initial structure both with and without the presence of plasma-induced excess electrons.

Adsorption of CO₂ on the supported Ni₅ cluster does not lead to a marked change in the shape of the cluster. Bond formation between the CO₂ molecule and Ni atoms of the cluster results in a bent structure of CO₂ (Figure 8a) with

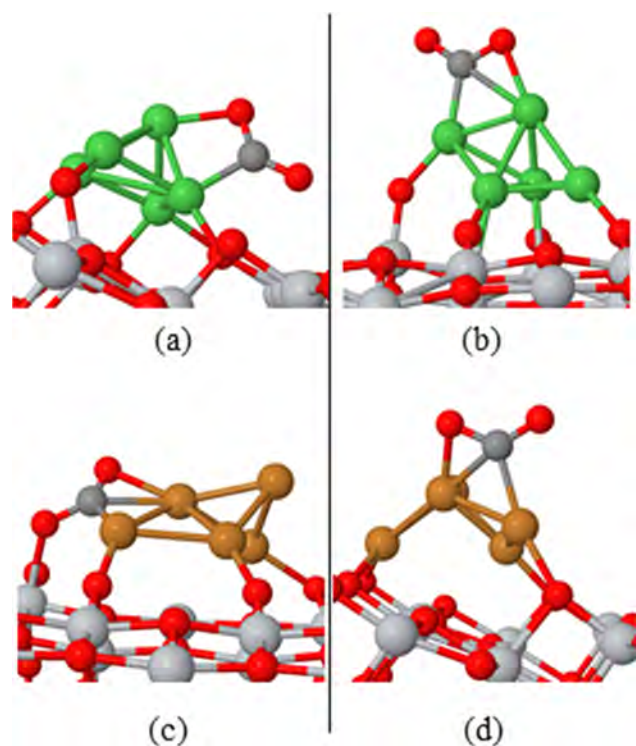


Figure 8. Adsorption of CO₂ on supported (a) Ni₅ neutral, (b) Ni₅ charged, (c) Cu₅ neutral, and (d) Cu₅ charged structures.

adsorption energies of -0.53 and -0.31 eV using DFT and DFT + *U*, respectively. During CO₂ adsorption, the net spin moment of the cluster remains at $3 \mu_B$, whereas its net charge increases from -0.893 *lel* to -1.412 *lel*, indicating the formation of a polar covalent bond between the cluster and the C atom of the CO₂ molecule. The Ni atom that bonds to C has a net charge of -0.730 *lel*, whereas the carbon atom has a charge of 1.769 *lel*.

Adsorption of CO₂ on the supported Cu₅ cluster results in a noticeable change in the cluster shape. In this case, CO₂ adsorbs on the interface via the C atom making bonds with two copper atoms of the cluster and the oxygen atom with a surface Ti atom (Figure 8c). In this configuration, the Cu₅ cluster has three coordinations with surface oxygens and three with the CO₂ molecule, while maintaining a net spin moment of 0 and having a partial net charge of -0.205 *lel*. The net charges of the carbon and the two Cu atoms of the cluster are 1.502 *lel*, -0.064 *lel*, and -0.228 *lel*, respectively. This shows the formation of a covalent bond between the cluster and the CO₂ molecule.

Bond lengths and adsorption energies of CO₂ on Ni₅ and Cu₅ clusters supported by anatase TiO₂(101) are shown in Table 2. From this table and also from Figure 9, we observe a noticeable improvement in the stability of the CO₂ molecule adsorbed on both clusters upon negatively charging the surface.

Table 2. Bond Lengths and Adsorption Energies of CO₂ Molecules on TiO₂-Supported Ni₅ and Cu₅ Clusters

method	structure	$r(\text{C}-\text{O})$	$\alpha(\text{OCO})$	E_{ads} (eV)
DFT	gas phase	1.17, 1.17	180	
	Ni ₅ neutral	1.22, 1.27	135.9	-0.53
	Ni ₅ charged	1.26, 1.32	124.2	-2.69
	Cu ₅ neutral	1.25, 1.28	131.0	-0.75
	Cu ₅ charged	1.25, 1.30	125.6	-1.57
DFT + <i>U</i>	Ni ₅ neutral	1.23, 1.27	134.3	-0.31
	Ni ₅ charged	1.26, 1.32	123.7	-2.53
	Cu ₅ neutral	1.25, 1.29	129.5	-0.64
	Cu ₅ charged	1.25, 1.29	125.8	-1.10

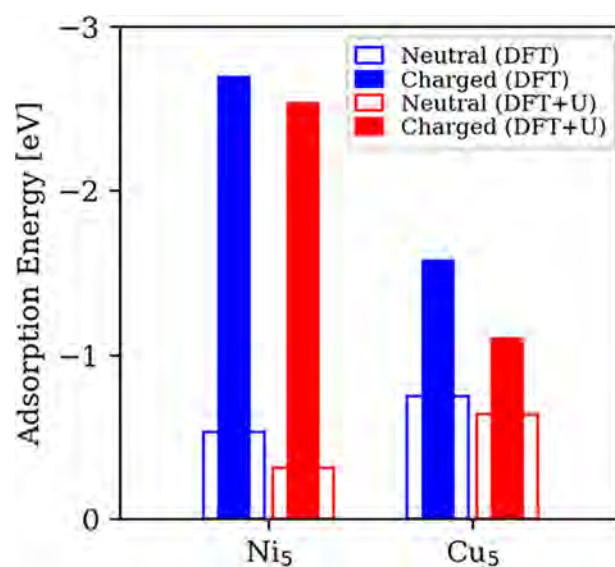


Figure 9. Adsorption energy of the CO₂ molecule on Ni₅/Cu₅ clusters supported by anatase TiO₂(101).

The increase in the adsorption energy in case of the charged Ni₅ structure is mostly because of the extra bond formation between the C atom and the top Ni atom of the cluster (Figure 8b). Together with a net spin moment of $2 \mu_B$, the net charge on the cluster increases to -1.708 *lel*, explaining the stronger bond between the cluster and the (positively charged) C atom of the molecule. The PDOS reveals that upon charging, there is

a shift in bonding states of the CO₂ molecule toward the valence band (Figure 10b). This leads to facilitation of the

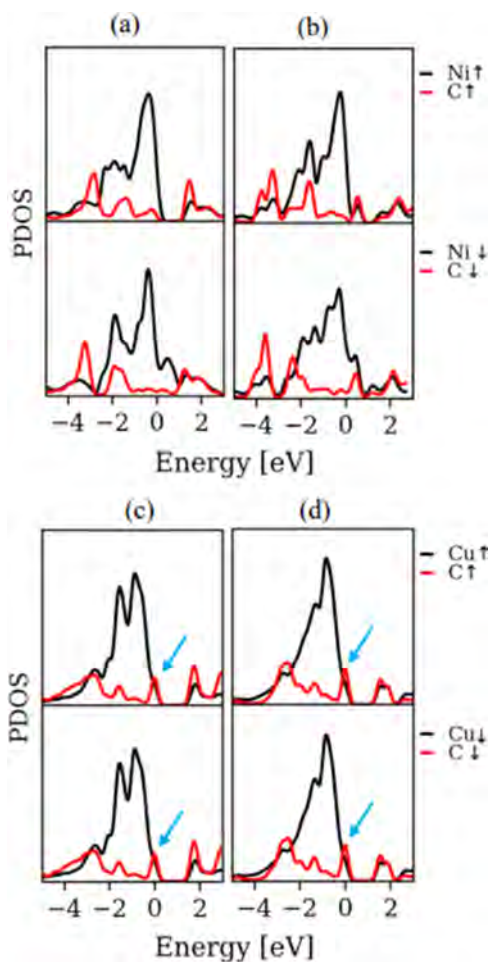


Figure 10. Projected density of states for the adsorption of the CO₂ molecule on TiO₂-supported (a) Ni₅ neutral, (b) Ni₅ charged, (c) Cu₅ neutral, and (d) Cu₅ charged structures.

hybridization of high-lying CO₂ antibonding π^* orbitals with d orbitals of the cluster. This shift is also seen in CO₂ adsorption on a negatively charged slab of titania, which resulted in the improved adsorption energy of the carbonate-like structure.

For CO₂ adsorption on the negatively charged Cu₅/TiO₂ (Figure 8d), we can see a slightly smaller band gap (Figure 10d), together with higher hybridization of C states with the cluster d orbitals. By analyzing the spin population and net charge of each atom, together with the morphological changes in the cluster shape upon charging the system, we can see that for the charged configuration, the CO₂ molecule binds only with the metal cluster, in contrast to the neutral case, in which CO₂ binds to the interface. This change in the adsorption mode is accompanied by a change in the amount of accumulated charge on the CO₂ molecule (from +0.184 |e| to -0.268 |e| upon negatively charging the system). The net spin moment remains 0, whereas the net charge on the cluster increases as a result of the presence of the excess electron. Considering the unpolarized spin configuration of the cluster, we conclude that the net charge of the cluster is actually the amount of charge that it shares with the surface as a result of their interaction. Thus, the improved adsorption energy of the CO₂ molecule on negatively charged Cu₅/TiO₂ is actually due

to more hybridization of the CO₂ states with the cluster's orbitals and also stronger interaction of the complex of cluster + molecule with the support's surface (considering that the amount of charge shared between the cluster and the support has been increased).

By looking into the bond lengths and angles reported in Table 2, we can see that the bond length elongation and bending of the O–C–O angle in the Ni₅ case are more sensitive to excess charge compared with the Cu₅ case. This agrees with the more stable bent structure of the CO₂ adsorbed on supported Ni₅.

Dissociated CO₂ on TiO₂, Ni₅/TiO₂, and Cu₅/TiO₂. In plasma catalysis, CO₂ dissociation can occur via several reaction paths. In this work, we focus on the adsorption of CO₂ on neutral and negatively charged surfaces and not on the actual reaction paths. Hence, these simulations do not aim to identify the most suitable catalyst for CO₂ dissociation, but they provide more insight into the effect of surface charging, which is one of the characteristic features of plasma catalysis distinguishing it from thermal catalysis. To estimate the effect of charge on the dissociation of CO₂, we examined various initial configurations of dissociated CO₂ (CO_(ads) + O_(ads)) on TiO₂, Ni₅/TiO₂, and Cu₅/TiO₂.

For CO₂ dissociation on neutral TiO₂, we did not find a stable structure for adsorbed CO_(ads). In most cases, CO either desorbs back in the gas phase or attracts an oxygen atom from the surface and so forms a linear CO₂ molecule. We have provided a less stable structure in Figure 11a, in which the CO_(ads) + O_(ads) phase is achieved. Although results in Figure 12 for dissociation on the bare surface of TiO₂ show an improvement in the adsorption energy due to the presence of the excess electron, dissociative adsorption is thermodynamically unfavorable, regardless of charging. This means that in the absence of a catalyst, dissociation of CO₂ on a bare slab of anatase will not proceed. An interesting parallel can be drawn with the effect of vacancies on the reactivity of TiO₂ toward CO₂ activation. Just like the formation of vacancies, electron addition effectively corresponds to a reduction of the TiO₂ surface. In both cases, this reduction has been found to result in an improved chemisorption of CO₂. However, vacancies additionally provide a strong binding site for oxygen,^{44,47} thus also promoting the dissociation of CO₂ adsorbed on a vacancy; such a site is not created upon charging, and CO₂ splitting remains unfavorable.

By employing Ni₅ as the catalyst, we find a dissociative adsorption energy of -0.03 eV for CO₂ dissociation on the neutral surface (Figure 11c). By adding an excess electron to the system, the adsorption energy significantly increases to -1.85 eV, which makes the reaction thermodynamically highly favorable (Figure 11d).

For the case of neutral Cu₅/TiO₂, dissociation of the CO₂ molecule into adsorbed (CO)_{ads} and (O)_{ads} is slightly endothermic with an adsorption energy of +0.14 eV (Figure 11e). Upon negatively charging the system (Figure 11f), the dissociative adsorption energy becomes -0.25 eV, making this reaction thermodynamically favorable. Figure 12 shows the corresponding dissociative adsorption energy for each configuration based on DFT and DFT + *U* calculations.

These results show that the presence of an excess electron has a positive impact on stabilization of the dissociated CO₂. This impact is more pronounced in case of a Ni pentamer as the catalyst, which shows excellent performance in response to the presence of a plasma-induced excess electron and

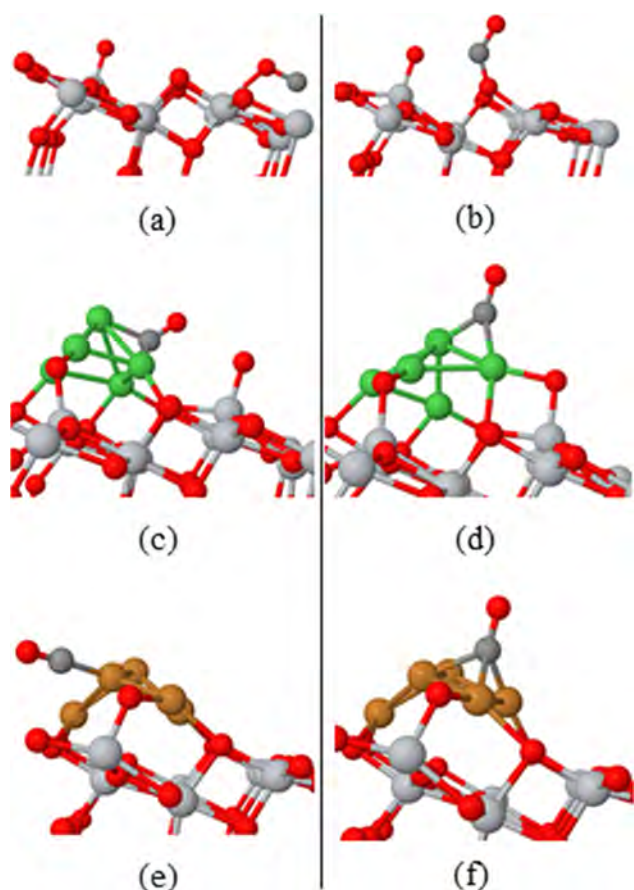


Figure 11. Most stable dissociated structures for CO_2 ($\text{CO}_{(\text{ads})} + \text{O}_{(\text{ads})}$) on (a) neutral TiO_2 , (b) charged TiO_2 , (c) neutral Ni_5/TiO_2 , (d) charged Ni_5/TiO_2 , (e) neutral Cu_5/TiO_2 , and (f) charged Cu_5/TiO_2 .

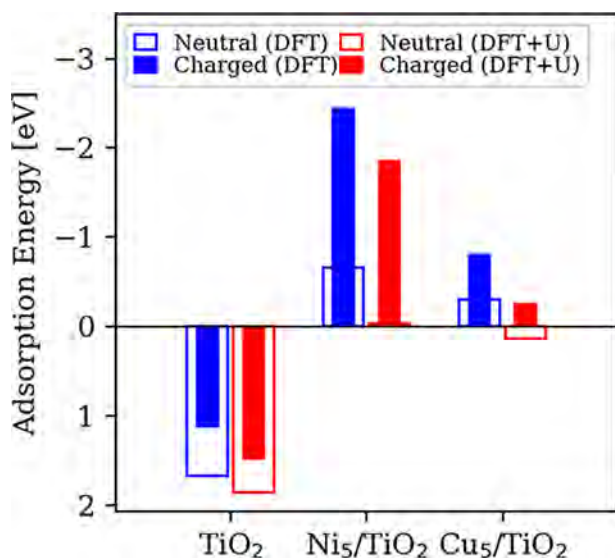


Figure 12. Dissociative adsorption energy of CO_2 on bare TiO_2 , Ni_5/TiO_2 , and Cu_5/TiO_2 .

significantly improves the adsorption energy of both adsorbed and dissociated CO_2 . Cu_5 adsorbed on a neutral TiO_2 surface is not active enough to dissociate the CO_2 in a favorable way, but it also shows positive feedback to negatively charging the surface. Therefore, these two particular test cases (adsorbed

Ni_5 and Cu_5) are good examples of how electrons from a nonequilibrium plasma can induce a shift in the chemical properties of different catalysts.

Although there are small differences in bond lengths and also adsorption energies in the results obtained from DFT and DFT + U , trends regarding the effect of charge on CO_2 activation are the same for both approaches. In addition to the comparison between the DFT and DFT + U results, we also investigated the effect of change in the surface charge density. We performed the same calculations for CO_2 adsorption on pristine titania by using a larger slab (2×4 supercell) of anatase $\text{TiO}_2(101)$ corresponding to a surface charge density of -0.05 C/m^2 , which is 2.7 times lesser than that of the small slab. The results indicate that for the large slab, the trends in the effect of charge on stabilization of the bent CO_2 molecule remain the same, although less pronounced (see the SI).

CONCLUSIONS

In this study, we investigated the effect of excess electrons induced by a plasma on the adsorption properties of Ni_5 and Cu_5 clusters over the anatase $\text{TiO}_2(101)$ surface and also CO_2 activation on both pristine a- TiO_2 and supported clusters.

Adsorption of Ni_5 and Cu_5 clusters on the surface of anatase (101) in the neutral case leads to a charge transfer between the cluster and the support. Depending on the type of catalyst, the direction of charge transfer can be from the surface to the cluster or vice versa. In this case, negatively charging the system leads to minor changes in the stabilization of the clusters. If the excess electron is localized on the surface, it will have a more pronounced impact than when the electron is localized on the cluster. Negatively charging the surface for adsorption of the CO_2 on a bare slab of anatase (101) causes the most stable structure of the CO_2 molecule to change from a linear to a bent configuration. This is mostly because of the shifting of the high-lying CO_2 antibonding π^* orbitals toward the valence band, facilitating their hybridization with p or d states of the surface.

In the case of employing Cu_5 and Ni_5 nanoclusters, the same result is seen for the improvement of bent CO_2 stabilization, although the underlying mechanisms are slightly different. Upon negatively charging the system in CO_2 adsorption on supported Ni_5 , the same shift in CO_2 high-lying states is seen, which leads to increased hybridization with the cluster d orbitals. In contrast, for the supported Cu_5 , changing the adsorption site from the interface to the cluster leads to more stabilization of the CO_2 molecule. This change in the adsorption mode results in a significant increase in the negative partial charge of the CO_2 molecule, which can be considered as indicative for activation of the molecule.⁴³

The dissociation of CO_2 on a bare slab of anatase titania is thermodynamically unfavorable, regardless of the added charge. CO_2 dissociation is favorable on Cu_5 as the catalyst in a charged configuration and on Ni_5 both in neutral and charged configurations. Together with better results for adsorption energy and bond elongation of the $\text{CO}_{2(\text{ads})}$ in charged configurations, Ni_5 could be a good option for plasma catalysis aiming at CO_2 conversion.

In general, plasma-induced excess electrons alter the adsorption process by shifting the antibonding states of CO_2 toward the valence band, increasing the polarization effects and changing the adsorption site of the molecule. These effects consequently lead to improved stabilization of bent (ads) and dissociated CO_2 in negatively charged structures. This can be

considered as a possible reason for the synergistic effects in plasma catalysis.

■ ASSOCIATED CONTENT

📄 Supporting Information

The Supporting Information is available free of charge on the ACS Publications website at DOI: 10.1021/acs.jpcc.8b11816.

Isolated Ni₅ and Cu₅ clusters, unstable structures for the Ni₅ and Cu₅ cluster adsorption on TiO₂ surface, PDOS plots for adsorption of clusters on TiO₂(101), results for structures with fixed bottom layers, calculations with a (2 × 4) supercell of TiO₂(101) (constrained and fully relaxed structures), and tables of spin moments and net charges (PDF)

■ AUTHOR INFORMATION

Corresponding Author

*E-mail: amin.jafarzadeh@uantwerpen.be. Tel: +32-32652360. Fax: +32-32652343.

ORCID

A. Jafarzadeh: 0000-0002-1638-6222

K. M. Bal: 0000-0003-2467-1223

A. Bogaerts: 0000-0001-9875-6460

E. C. Neyts: 0000-0002-3360-3196

Notes

The authors declare no competing financial interest.

■ ACKNOWLEDGMENTS

The authors acknowledge financial support from the TOP research project of the Research Fund of the University of Antwerp (grant ID: 32249). K.M.B. was funded as a Ph.D. fellow (aspirant) of the FWO-Flanders (Research Foundation-Flanders), Grant 11V8915N. The computational resources and services used in this work were provided by the VSC (Flemish Supercomputer Center), funded by the FWO and the Flemish Government—Department EWI.

■ REFERENCES

- Neyts, E. C.; Bogaerts, A. Understanding plasma catalysis through modelling and simulation-A review. *J. Phys. D: Appl. Phys.* **2014**, *47*, No. 224010.
- Neyts, E. C.; Ostrikov, K. K.; Sunkara, M. K.; Bogaerts, A. Plasma Catalysis: Synergistic Effects at the Nanoscale. *Chem. Rev.* **2015**, *115*, 13408–13446.
- Kim, H.-H.; Ogata, A.; Schiorlin, M.; Marotta, E.; Paradisi, C. Oxygen Isotope (18O2) Evidence on the Role of Oxygen in the Plasma-Driven Catalysis of VOC Oxidation. *Catal. Lett.* **2011**, *141*, 277–282.
- Maciuca, A.; Batiot-Dupeyrat, C.; Tatibouet, J.-M. Synergetic effect by coupling photocatalysis with plasma for low VOCs concentration removal from air. *Appl. Catal., B* **2012**, *125*, 432–438.
- Jögi, I.; Erme, K.; Haljaste, A.; Laan, M. Oxidation of nitrogen oxide in hybrid plasma-catalytic reactors based on DBD and Fe2O3*. *Eur. Phys. J.: Appl. Phys.* **2013**, *61*, No. 24305.
- Mizuno, A. Generation of non-thermal plasma combined with catalysts and their application in environmental technology. *Catal. Today* **2013**, *211*, 2–8.
- Tatarova, E.; Bundaleska, N.; Sarrette, J. P.; Ferreira, C. M. Plasmas for environmental issues: from hydrogen production to 2D materials assembly. *Plasma Sources Sci. Technol.* **2014**, *23*, No. 063002.
- Kim, H.-H.; Teramoto, Y.; Ogata, A.; Takagi, H.; Nanba, T. Plasma Catalysis for Environmental Treatment and Energy Applications. *Plasma Chem. Plasma Process.* **2016**, *36*, 45–72.
- Lee, H.; Sekiguchi, H. Plasma-catalytic hybrid system using spouted bed with a gliding arc discharge: CH₄ reforming as a model reaction. *J. Phys. D: Appl. Phys.* **2011**, *44*, No. 274008.
- Tu, X.; Gallon, H. J.; Twigg, M. V.; Gorry, P. A.; Whitehead, J. C. Dry reforming of methane over a Ni/Al₂O₃ catalyst in a coaxial dielectric barrier discharge reactor. *J. Phys. D: Appl. Phys.* **2011**, *44*, No. 274007.
- Zhang, L.; ling Sha, X.; Zhang, L.; bin He, H.; hua Ma, Z.; wei Wang, L.; xin Wang, Y.; xia She, L. Synergistic catalytic removal NOX and the mechanism of plasma and hydrocarbon gas. *AIP Adv.* **2016**, *6*, No. 075015.
- Mei, D.; Yan, J.; Tu, X. In *Plasma-Catalytic Conversion of CO₂ into Value-Added Chemicals: Understanding the Synergistic Effect at Low Temperatures*, 2015 IEEE International Conference on Plasma Sciences; IEEE, 2015.
- Kim, J.; Go, D. B.; Hicks, J. C. Synergistic effects of plasma-catalyst interactions for CH₄ activation. *Phys. Chem. Chem. Phys.* **2017**, *19*, 13010–13021.
- Zhou, R.; Zhou, R.; Zhang, X.; Li, J.; Wang, X.; Chen, Q.; Yang, S.; Chen, Z.; Bazaka, K.; Ostrikov, K. Synergistic Effect of Atmospheric-pressure Plasma and TiO₂ Photocatalysis on Inactivation of *Escherichia coli* Cells in Aqueous Media. *Sci. Rep.* **2016**, *6*, No. 39552.
- Nørskov, J. Electronic factors in catalysis. *Prog. Surf. Sci.* **1991**, *38*, 103–144.
- Holzer, F.; Roland, U.; Kopinke, F.-D. Combination of non-thermal plasma and heterogeneous catalysis for oxidation of volatile organic compounds: Part 1. Accessibility of the intra-particle volume. *Appl. Catal., B* **2002**, *38*, 163–181.
- Durme, J. V.; Dewulf, J.; Sysmans, W.; Leys, C.; Langenhove, H. V. Efficient toluene abatement in indoor air by a plasma catalytic hybrid system. *Appl. Catal., B* **2007**, *74*, 161–169.
- Shirazi, M.; Bogaerts, A.; Neyts, E. C. A DFT study of H-dissolution into the bulk of a crystalline Ni(111) surface: a chemical identifier for the reaction kinetics. *Phys. Chem. Chem. Phys.* **2017**, *19*, 19150–19158.
- Shirazi, M.; Neyts, E. C.; Bogaerts, A. DFT study of Ni-catalyzed plasma dry reforming of methane. *Appl. Catal., B* **2017**, *205*, 605–614.
- Chen, H.-Y. T.; Tosoni, S.; Pacchioni, G. Adsorption of Ruthenium Atoms and Clusters on Anatase TiO₂ and Tetragonal ZrO₂(101) Surfaces: A Comparative DFT Study. *J. Phys. Chem. C* **2015**, *119*, 10856–10868.
- Puigdollers, A. R.; Schlexer, P.; Pacchioni, G. Gold and Silver Clusters on TiO₂ and ZrO₂ (101) Surfaces: Role of Dispersion Forces. *J. Phys. Chem. C* **2015**, *119*, 15381–15389.
- Tosoni, S.; Chen, H.-Y. T.; Pacchioni, G. A DFT study of Ni clusters deposition on titania and zirconia (101) surfaces. *Surf. Sci.* **2016**, *646*, 230–238.
- Liu, C.; Yang, B.; Tyo, E.; Seifert, S.; DeBartolo, J.; von Issendorff, B.; Zapol, P.; Vajda, S.; Curtiss, L. A. Carbon Dioxide Conversion to Methanol over Size-Selected Cu₄ Clusters at Low Pressures. *J. Am. Chem. Soc.* **2015**, *137*, 8676–8679.
- Fuzhen, Z.; Miao, G.; Kun, C.; Yuhua, Z.; Jinlin, L.; Rong, C. Atomic Layer Deposition of Ni on Cu Nanoparticles for Methanol Synthesis from CO₂ Hydrogenation. *ChemCatChem* **2017**, *9*, 3772–3778.
- Diebold, U.; Ruzycki, N.; Herman, G.; Selloni, A. One step towards bridging the materials gap: surface studies of TiO₂ anatase. *Catal. Today* **2003**, *85*, 93–100.
- Li, Y.-F.; Selloni, A. Theoretical Study of Interfacial Electron Transfer from Reduced Anatase TiO₂(101) to Adsorbed O₂. *J. Am. Chem. Soc.* **2013**, *135*, 9195–9199.
- VandeVondele, J.; Krack, M.; Mohamed, F.; Parrinello, M.; Chassaing, T.; Hutter, J. Quickstep: Fast and accurate density functional calculations using a mixed Gaussian and plane waves approach. *Comput. Phys. Commun.* **2005**, *167*, 103–128.

- (28) Hutter, J.; Iannuzzi, M.; Schiffmann, F.; VandeVondele, J. cp2k: atomistic simulations of condensed matter systems. *Wiley Interdiscip. Rev.: Comput. Mol. Sci.* **2013**, *4*, 15–25.
- (29) VandeVondele, J.; Hutter, J. Gaussian basis sets for accurate calculations on molecular systems in gas and condensed phases. *J. Chem. Phys.* **2007**, *127*, No. 114105.
- (30) Goedecker, S.; Teter, M.; Hutter, J. Separable dual-space Gaussian pseudopotentials. *Phys. Rev. B: Condens. Matter Mater. Phys.* **1996**, *54*, 1703–1710.
- (31) Krack, M. Pseudopotentials for H to Kr optimized for gradient-corrected exchange-correlation functionals. *Theor. Chem. Acc.* **2005**, *114*, 145–152.
- (32) Perdew, J. P.; Burke, K.; Ernzerhof, M. Generalized Gradient Approximation Made Simple. *Phys. Rev. Lett.* **1996**, *77*, 3865–3868.
- (33) Grimme, S.; Antony, J.; Ehrlich, S.; Krieg, H. A consistent and accurate ab initio parametrization of density functional dispersion correction (DFT-D) for the 94 elements H-Pu. *J. Chem. Phys.* **2010**, *132*, No. 154104.
- (34) Grimme, S.; Ehrlich, S.; Goerigk, L. Effect of the damping function in dispersion corrected density functional theory. *J. Comput. Chem.* **2011**, *32*, 1456–1465.
- (35) Bultinck, P.; Alsenoy, C. V.; Ayers, P. W.; Carbo-Dorca, R. Critical analysis and extension of the Hirshfeld atoms in molecules. *J. Chem. Phys.* **2007**, *126*, No. 144111.
- (36) Howard, C. J.; Sabine, T. M.; Dickson, F. Structural and thermal parameters for rutile and anatase. *Acta Crystallogr., Sect. B: Struct. Sci.* **1991**, *47*, 462–468.
- (37) Bal, K. M.; Huygh, S.; Bogaerts, A.; Neyts, E. C. Effect of plasma-induced surface charging on catalytic processes: application to CO₂ activation. *Plasma Sources Sci. Technol.* **2018**, *27*, No. 024001.
- (38) Martyna, G. J.; Tuckerman, M. E. A reciprocal space based method for treating long range interactions in ab initio and force-field-based calculations in clusters. *J. Chem. Phys.* **1999**, *110*, 2810–2821.
- (39) Bal, K. M.; Neyts, E. C. Modelling Molecular Adsorption on Charged or Polarized Surfaces: a Critical Flaw in Common Approaches. *Phys. Chem. Chem. Phys.* **2018**, *20*, 8456–8459.
- (40) Anisimov, V. I.; Zaanen, J.; Andersen, O. K. Band theory and Mott insulators: Hubbard U instead of Stoner I. *Phys. Rev. B* **1991**, *44*, 943–954.
- (41) Dudarev, S. L.; Botton, G. A.; Savrasov, S. Y.; Humphreys, C. J.; Sutton, A. P. Electron-energy-loss spectra and the structural stability of nickel oxide: An LSDA + U study. *Phys. Rev. B* **1998**, *57*, 1505–1509.
- (42) Hahn, K. R.; Seitsonen, A. P.; Iannuzzi, M.; Hutter, J. Functionalization of CeO₂(111) by Deposition of Small Ni Clusters: Effects on CO₂ Adsorption and O Vacancy Formation. *ChemCatChem* **2015**, *7*, 625–634.
- (43) Iyemperumal, S. K.; Deskins, N. A. Activation of CO₂ by supported Cu clusters. *Phys. Chem. Chem. Phys.* **2017**, *19*, 28788–28807.
- (44) Sorescu, D. C.; Al-Saidi, W. A.; Jordan, K. D. CO₂ adsorption on TiO₂(101) anatase: A dispersion-corrected density functional theory study. *J. Chem. Phys.* **2011**, *135*, No. 124701.
- (45) Zhang, Q.-Z.; Wang, W.-Z.; Bogaerts, A. Importance of surface charging during plasma streamer propagation in catalyst pores. *Plasma Sources Sci. Technol.* **2018**, *27*, No. 065009.
- (46) Deskins, N. A.; Liu, C.; Iyemperumal, S. K.; Li, G. Photocatalytic CO₂ reduction by highly dispersed Cu sites on TiO₂. *J. Photonics Energy* **2016**, *7*, No. 012004.
- (47) Huygh, S.; Bogaerts, A.; Neyts, E. C. How Oxygen Vacancies Activate CO₂ Dissociation on TiO₂ Anatase (001). *J. Phys. Chem. C* **2016**, *120*, 21659–21669.